

Molecular elimination of Br₂ in 248 nm photolysis of bromoform probed by using cavity ring-down absorption spectroscopy

Hong-Yi Huang, Wan-Ting Chuang, Ramesh C. Sharma, Ching-Yi Hsu, and King-Chuen Lin*

Department of Chemistry, National Taiwan University, Taipei, Taiwan and Institute of Atomic and Molecular Sciences, Taipei 106, Taiwan

Ching-Han Hu

Department of Chemistry, National Changhua University of Education, Changhua 500, Taiwan

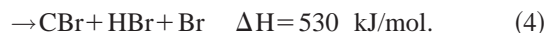
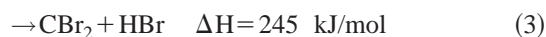
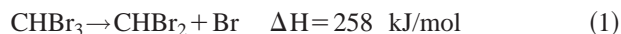
(Received 14 April 2004; accepted 7 June 2004)

By using cavity ring-down spectroscopy technique, we have observed the channel leading to Br₂ molecular elimination following photodissociation of bromoform at 248 nm. A tunable laser beam, which is crossed perpendicular to the photolysis laser beam in a ring-down cell, is used to probe the Br₂ fragment in the $B^3\Pi_{ou}^+ - X^1\Sigma_g^+$ transition using the range 515–524 nm. The ring-down time lasts 500 ns, so the rotational population of the Br₂ fragment may not be nascent nature, but its vibrational population should be. The vibrational population ratio of Br₂($v=1$)/Br₂($v=0$) = 0.8 ± 0.2 implies that the fragmented Br₂ is vibrationally hot. The quantum yield of the molecular elimination reaction is 0.23 ± 0.05 , consistent with the values of 0.26 and 0.16 reported in 234 and 267 nm photolysis of bromoform, respectively, using velocity ion imaging. A plausible photodissociation pathway is proposed, based upon this work and *ab initio* calculations. The \tilde{A}^1A_2 , \tilde{B}^1E , and \tilde{C}^1A_1 singlet states of bromoform are probably excited at 248 nm. These excited states may couple to the high vibrational levels of the ground state \tilde{X}^1A_1 via internal conversion. This vibrationally excited bromoform readily surpasses a reaction barrier 389.6 kJ/mol prior to decomposition. The transition state structure tends to correlate with vibrationally hot Br₂. Dissociation after internal conversion of the excited states to vibrationally excited ground state should result in a large fraction of the available energy to be partitioned in vibrational states of the fragments. The observed vibrationally hot Br₂ fragment seems to favor the dissociation pathway from high vibrational levels of the ground state. Nevertheless, the other reaction channel leading to a direct impulsive dissociation from the excited states cannot be excluded. © 2004 American Institute of Physics. [DOI: 10.1063/1.1777211]

I. INTRODUCTION

The atmospheric chemistry of bromine has recently received considerable attention. In spite of the low concentration of bromine in the atmosphere, its catalytic rate on depletion stratosphere ozone is proposed up to be 100 times more rapid than chlorine atoms.¹ In addition, the coupling of BrO and ClO cycles to produce the atomic forms of Br and Cl can enhance the ozone depletion by chlorofluorocarbons up to 20%. Halons and methyl bromides are well known sources of atmospheric bromine.^{2,3} Bromoform, which can last long in the atmosphere and is primarily biogenic in origin, is another source that can contribute to active bromine.^{4,5} Photodissociation is considered as the major mechanism for bromoform removal from the atmosphere, but the knowledge of its photochemistry is very limited.

In CHBr₃ photolysis, four dissociation channels are thermodynamically probable in the ultraviolet wavelength region:



Early in 1961, Simons and Yarwood studied the photodissociation of CHBr₃ using flash photolysis near 200 nm.⁶ They ascribed the observation of CBr to the primary loss of Br atom followed by decomposition of the energized CHBr₂ radical. By using photofragment translational spectroscopy, McGivern *et al.* suggested that the loss of bromine atom is the only primary channel in the 193 nm photolysis, while the remaining CHBr₂ may undergo secondary dissociation to give rise to comparable yield for the HBr elimination and CBr bond cleavage.⁷ On the other hand, Xu *et al.* using a velocity ion-imaging detection first observed a channel for the elimination of molecular bromine in the 234 and 267 nm photolysis of bromoform, and reported a quantum yield of 0.26 and 0.16, respectively.⁸ Such an observation has an important impact on the chemistry of atmospheric bromine, where the current atmospheric photochemical models consider only the loss of bromine atom.

*Author to whom correspondence should be addressed. Fax: 886-2-23621483; electronic mail: kclin@ccms.ntu.edu.tw

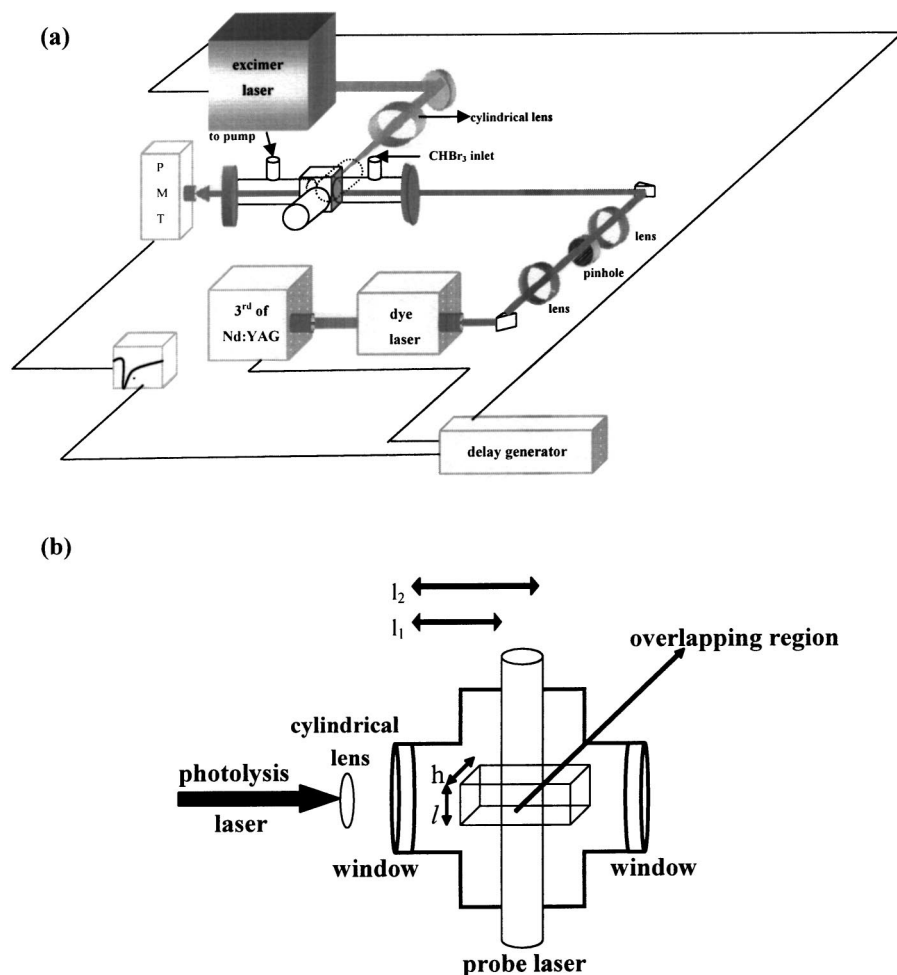


FIG. 1. Schematic of experimental apparatus for cavity ring-down absorption spectroscopy.

The present work aims to confirm the photodissociation mechanism of bromoform to produce the Br₂ fragment by using a cavity ring-down absorption spectroscopy (CRDS). This technique has been widely applied in the studies of spectroscopy, kinetics, dynamics, and photochemistry in the condensed or gas phases.^{9–13} The method is based upon the measurement of the decay rate of light trapped in an optical cavity with high reflectance. When a pulsed laser radiation is guided into an optical cavity, formed by a pair of highly reflective mirrors ($R > 99.9\%$), the small amount of light trapped inside the cavity reflects between two mirrors with a small fraction transmitting through each mirror for each pass. The decay rate of the light leaking out of the cavity is related to the absorption coefficient of the sample in the cavity. As an emerging absorption technique, CRDS has the following advantages: (1) independence of fluctuation of radiation intensity; (2) more sensitivity than conventional absorption methods due to a longer optical path; and (3) ease to set up apparatus.¹⁴

In this work, we adopt the CRDS technique to measure the nascent vibrational spectra of the molecular bromine fragmented in the photodissociation of bromoform. An excimer laser at 248 nm is employed to dissociate bromoform in a ring-down cell, while the other tunable laser is used to probe the Br₂ fragment. Given the absorbed photon number density and the Br₂ concentration produced in the beam-crossed region, the quantum yield for the molecular elimina-

tion channel is estimated to be 0.23 ± 0.05 , which is consistent with those reported by Xu *et al.* using velocity ion-imaging detection.⁸ The vibrational branching ratio of Br₂($v=1$) to Br₂($v=0$) is determined to be 0.8 ± 0.2 , suggesting that the Br₂ fragment is vibrationally hot. With the aid of *ab initio* potential energy calculations, the dissociation mechanism leading to the products of Br₂ and CHBr may be gained insight.

II. EXPERIMENTAL SETUP

The CRDS apparatus used for photodissociation study of bromoform is depicted in Fig. 1. The radiation sources are composed of an excimer laser emitting at 248 nm for photolysis of CHBr₃ and a tunable dye laser working on Coumarin 503 dye (515–524 nm), pumped by the second harmonic of Nd:YAG laser, used to probe the released Br₂ fragment in the $B^3\Pi_{ou}^+ \leftarrow X^1\Sigma_g^+$ transition. The photolysis and probe lasers, with pulse durations about 20 and 5–8 ns, respectively, both were operated at repetition rates of 10 Hz. The photolysis laser was focused with a 25 cm focal length cylindrical lens onto the ring-down cell at right angle to the cavity, while the probe beam was injected along the axis of the cavity. The two laser beams were overlapped in the center of the flow cell. The volume of the overlapping region was evaluated by multiplication of the beam width and height of the photolysis laser and the beam diameter of the

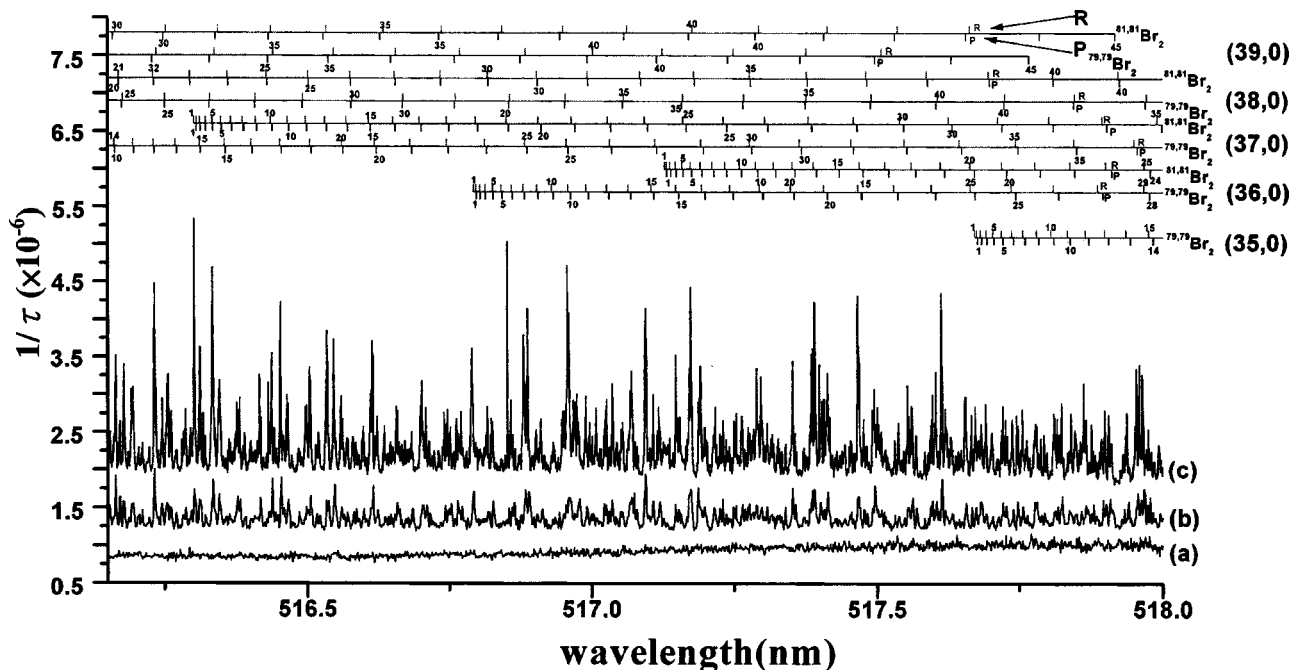


FIG. 2. CRDS spectra of Br_2 obtained from photolysis of bromoform at pressure of 2 Torr (a) without use of photolysis laser and (b) with use of photolysis laser. (c) CARD spectra of pure Br_2 compound at pressure of 72 mTorr.

probe laser, corresponding to $(18 \times 1 \times 3) \pm 5 \text{ mm}^3$. The delay time between photolysis and probe laser was adjusted to be 20 ns. In order to remain mostly the TEM_{00} mode, the probe beam was guided through a spatial filter made of a pair of lenses of 10 and 5 cm focal length and a pinhole with $70 \mu\text{m}$ diameter. The pulse energies for photolysis and probe laser were controlled at 20 ± 1 and $4 \pm 0.2 \text{ mJ}$, respectively, prior to entering the ring-down cell.

In this work, we used CHBr_3 , CCl_3Br , and CH_2ClBr as photolysis reagents. The later two were used to check whether the recombination process between primary Br-atom fragments played a significant role during the long ring-down time. They were all purified by repeated freeze-pump-thaw cycles at 77 K and each individual was introduced in the ring-down cell with the pressure regulated at 1–2 Torr monitored by an mks pressure gauge. The ring-down cell was sealed with two mirrors with high reflectance $>99.9\%$ at 500 nm, a diameter of 25.4 mm and a radius of curvature of 1 m. The probe beam was injected through the front mirror into the ring-down cell, but only a small fraction could be coupled into the cavity by transmission through one of cavity end mirrors. The mirrors were mounted about 53 cm apart in such a way that their positions may be slightly adjusted to trap a laser pulse inside the cavity by ensuring it retroreflects back and forth between two mirrors. A photomultiplier tube was positioned behind the rear mirror to record the intensity of the light pulse leaking out of the mirror on each round trip inside the cavity. The intensity envelope composed of each transmitted pulse exhibits an exponential decay, because of a constant loss of light at each mirror surface. The temporal profile of the ring-down signal was recorded on a transit digitizer and transferred to a personal computer. The ring-down time for each laser pulse may be determined by a best fit of the acquired exponential decay. The Br_2 absorption

spectra were obtained by scanning the wavelength of the probe laser with a spectral resolution of 0.1 cm^{-1} .

III. POTENTIAL ENERGY CALCULATIONS

The excitation of CHBr_3 at 248 nm is lower in energy than that of the vertical transition to its first excited singlet state \tilde{A}^1A_2 .¹⁵ Stationary points on the ground state potential energy surface were located using the B3LYP density functional theory with the 6-311G** basis set.^{16,17} Unrestricted computations were performed throughout this work. For the transition states (TSs), intrinsic reaction coordinate calculations were performed.¹⁸ The computations were carried out with the GAUSSIAN 98 suite of programs.¹⁹

We have located a secondary saddle point (TS1) on the PES at 389.6 kJ/mol above the CHBr_3 minimum, and a genuine TS (TS2) which lies at 195.8 kJ/mol. TS1 (C_s) has an $\langle S^2 \rangle$ of 0.939 and two imaginary vibrational frequencies at 273 and 84 cm^{-1} , which correspond to symmetric and asymmetric C-Br stretchings, respectively. The symmetric stretching mode leads to $\text{CHBr} + \text{Br}_2$ (327.0 kJ/mol). TS2 ($\langle S^2 \rangle = 0$) has an imaginary frequency at 261 cm^{-1} , which corresponds to C-Br bond breaking, leading to the $\text{CHBr}_2 \cdots \text{Br}$ intermediate IN (172.1 kJ/mol), which further dissociates into $\text{CHBr}_2 + \text{Br}$. The $\text{Br} \cdots \text{Br}$ distance in the intermediate is 2.719 \AA .

IV. RESULTS AND DISCUSSION

A. Nascent vibrational distribution of Br_2 fragment

As shown in Fig. 2, the CRDS spectra of Br_2 fragment in the $B^3\Pi_{ou}^+ \leftarrow X^1\Sigma_g^+$ transition are obtained following photodissociation of bromoform at 248 nm. The Br_2 spectral assignment is referred to the report by Barrow *et al.*²⁰ Part of

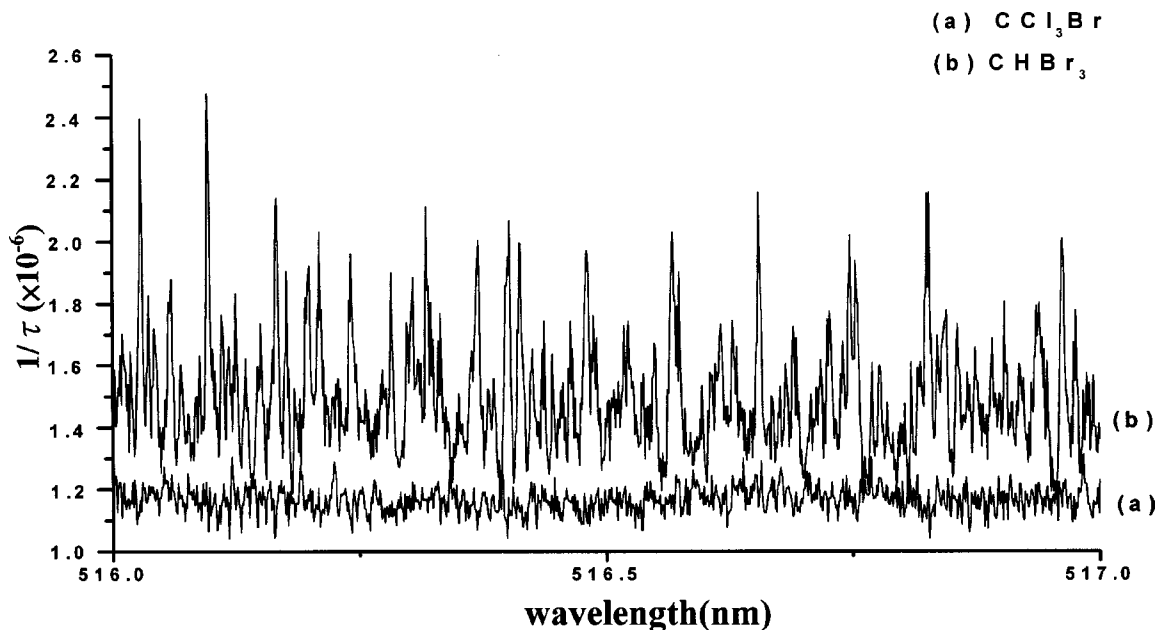


FIG. 3. Detection of CRDS spectra of Br_2 following photolysis of (a) CCl_3Br and (b) CHBr_3 at 248 nm.

the results are shown in Fig. 2. When the photolysis laser is off, the Br_2 signal disappears [Fig. 2(a)]. To confirm the acquired spectra resulting from the Br_2 fragment, a pure Br_2 compound at 72 mTorr was substituted in the cell and its CRDS signal was also measured for comparison [Fig. 2(c)]. Consistency of the spectra between Figs. 2(b) and 2(c) reveals only the Br_2 fragment occurring in the 515–524 nm region in the photolysis of bromoform.

When the photolysis-probe delay time is varied from 20 to 100 ns, the rotational feature of Br_2 remains the same. Since the ring-down time is long, about 500 ns, the rotational population becomes thermally equilibrated and probably loses its nascent nature. Nevertheless, the occurrence of vibrational energy transfer takes a longer time such that the vibrational population detected by CRDS method may still be in a nascent state. The vibrational population amounts to summation of each rotational line of the corresponding level. The rotational lines of *P* and *R* branches in the bands (37,0) and (41,1) both have been assigned up to $J=34$. To estimate the branching ratio of vibrational populations in the $v=0$ and 1 levels, one must take into account Franck-Condon factors of the bands (37,0) and (41,1) and Hönl-London factor for each rotational line.²¹ The ratio of $\text{Br}_2(v=1)/\text{Br}_2(v=0)$ yields a value of 0.8 ± 0.2 , which bears a large uncertainty caused by ignorance of the rotational lines $>J=34$ and the partial overlap between them. In spite of that, the branching ratio shows significant evidence that the Br_2 fragment is vibrationally hot following photodissociation of bromoform.

During a long ring-down time, is it probable that the Br_2 fragment comes from the secondary recombination of two Br atoms resulting from the dissociation channel (1)? We carried out two experiments to verify this possibility. First, a precursor CH_2ClBr or CCl_3Br was used to replace CHBr_3 in the cell. Under otherwise identical conditions, Fig. 3 shows no detectable signals of Br_2 fragment in the photolysis of the

mono-Br-containing molecules. Even when the sample pressure was increased to 2.5 Torr and the photolysis-probe delay time was extended to 80 ns, we could not find any detectable bromine molecules either. Second, the measurement of laser energy dependence was performed for a selective rotational line *P*(37) of the band (35,0) at 519.68 nm. The plot of rotational intensity as a function of the laser energy in a logarithmic scale yields a straight line with a slope equal to one, indicating that only single photon is involved in the formation of bromine molecule. Two photons are otherwise required for the recombination process.

This work demonstrates for the first time using CRD absorption spectroscopy that Br_2 is formed in the primary photodissociation of bromoform at 248 nm. When laser wavelength is changed to 266 nm, the CRDS signals for Br_2 are also detected but it is weaker under otherwise identical conditions. However, when a laser-induced fluorescence (LIF) technique was employed, we failed to find any detectable signals from *B* to *X* transition of Br_2 fragment in the primary dissociation channel at a pressure of 8 Torr CHBr_3 and with a photolysis-probe delay time of 150 ns. As the delay time is prolonged to 150 ns, only a Swan band of C_2 appears in the 516–517 nm region.²² When a pure Br_2 compound is substituted for bromoform, the LIF signals of the rotation lines in the (37,0) band appear to be twice as wide when compared to those detected by CRDS method. The difficulty with LIF detection may rise from a low fluorescence quantum yield caused by predissociation with the repulsive $C^1\Pi_{1u}$ state.^{23,24}

B. Quantum yield for Br_2 elimination

The quantum yield for the CHBr_3 photolysis via channel (2) can be determined from the ratio of Br_2 concentration produced in the beam-crossed region of photolysis/probe la-

sers to the photon number density absorbed in the same region. The absorbed photon number density ϕ is evaluated by using the following equation:

$$\phi = \frac{E_{in} - E_{out}}{h\nu\Delta V}, \quad (5)$$

where h denotes the Planck's constant, ν denotes radiation frequency, ΔV denotes the beam-crossed region, and E_{in} and E_{out} indicate the photon energy of the incoming and outgoing radiation for photolysis. E_{in} and E_{out} may be estimated by using Lambert-Beer's law, as expressed by

$$E_{in} = E_0 \exp(-\sigma n \ell_1), \quad (6)$$

$$E_{out} = E_0 \exp(-\sigma n \ell_2), \quad (7)$$

where E_0 is the photon energy of incident photolysis laser pulse prior to the cell, σ is the absorption cross section of CHBr_3 , n is the number density of CHBr_3 in the cell, and ℓ_1 (or ℓ_2) indicates the distance between the inner side of the entrance cell window and the front (or rear) edge of the beam-crossed region. The schematic is depicted in Fig. 1(b). σ is reported to be $1.94 \times 10^{-18} \text{ cm}^2$ at 248 nm.²⁵ ℓ_1 and ℓ_2 are measured to be 6.35 ± 0.02 and 6.65 ± 0.02 cm, respectively. The number density of CHBr_3 in the cell is $4 \times 10^{16} \text{ molecule/cm}^3$. The beam-crossed region is estimated to be $(5.4 \pm 0.5) \times 10^{-2} \text{ cm}^3$.

The Br_2 concentration may be determined by measuring its absorption coefficient after photolysis. The absorption coefficient α is evaluated by the following equation:

$$\alpha = \frac{d}{cl} \left(\frac{1}{\tau} - \frac{1}{\tau_0} \right), \quad (8)$$

where $d = 53$ cm, the distance between two high reflectance mirrors; $l = 1.8$ cm, the optical length of the absorber; c is the light speed, and τ and τ_0 are the ring-down times of Br_2 as a result of the probe laser wavelength in-resonance or off-resonance with 519.68 nm, respectively. If an empty cavity is used for the measurement, the additional bound-free absorption may contribute to error in determining the term $(1/\tau - 1/\tau_0)$. In this work the photolysis-probe delay time is set at 20 ns which are short enough to ignore the diffusion loss of Br_2 fragment. Given the absorption cross section of the Br_2 vapor at 519.68 nm, its concentration may be readily obtained.

To determine the absorption cross section of Br_2 , we replace the precursor with the pure Br_2 compound regulated at different vapor pressures in the flow cell. The corresponding ring-down times τ and τ_0 were measured using the probe laser alone, as tuned in-resonance or off-resonance with 519.68 nm, respectively. By using Eq. (8) in which l is replaced by d , the absorption coefficient for a given vapor pressure may be obtained. As shown in Fig. 4, the linear plot of the absorption coefficient against the number density of Br_2 has a slope that is equal to the absorption cross section, $\sigma_{\text{Br}_2} = (1.3 \pm 0.3) \times 10^{-19} \text{ cm}^2$. The Br_2 concentration produced in the interaction region may be evaluated from the ratio of $\alpha/\sigma_{\text{Br}_2}$.

When the photolysis beam energies are varied from 10.7, 22.4, and 25.4 mJ/pulse, the methods described above may

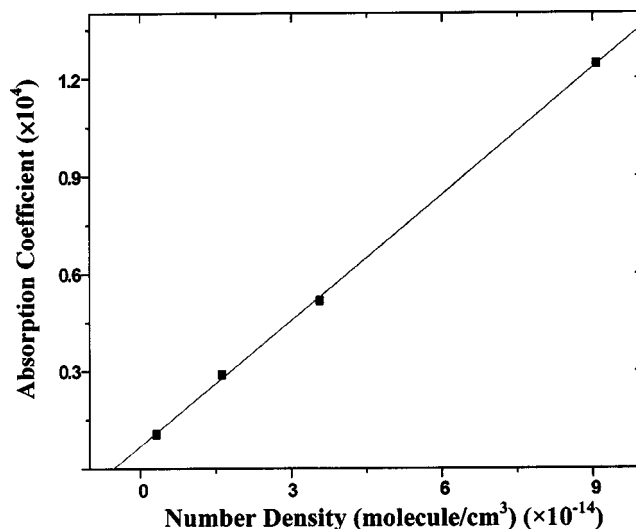


FIG. 4. Plot of absorption coefficient versus number density of Br_2 at laser wavelength of 519.68 nm, yielding a slope indicative of the corresponding absorption cross section $(1.3 \pm 0.3) \times 10^{-19} \text{ cm}^2$.

be used to obtain corresponding photon number density and Br_2 concentrations. These two parameters are linearly proportional to each other. A plot of these quantities yields a straight line whose slope is equal to the quantum yield of 0.23 ± 0.05 for the molecular elimination channel (Fig. 5). Our result is consistent with those reported by Jackson group using velocity ion-imaging detection.⁸ They obtained the quantum yields of 0.26 and 0.16 at 234 and 267 nm, respectively, by assuming the ionization cross sections were identical between the two fragment ions CHBr and CH_2Br^+ . Thus far, the dissociation channels (1) and (2) have ever been observed with short wavelength radiation. The quantum yield for the other primary channel leading to CHBr_2 and Br should be 0.77. The branching ratio of dissociation channels (1) to (2) is about 3:1. Therefore, the molecular elimination of Br_2 must play a significant role in the atmospheric chem-

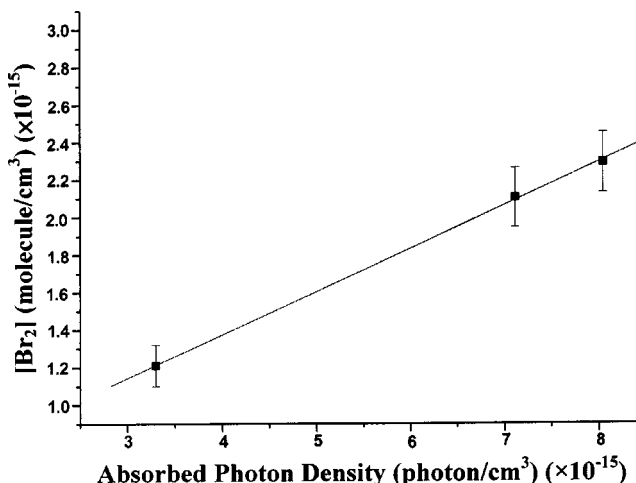


FIG. 5. Plot of number density of Br_2 produced in 248 nm photolysis of bromoform against the absorbed photon density, yielding a slope indicative of quantum yield 0.23 ± 0.05 for the dissociation channel of molecular elimination.

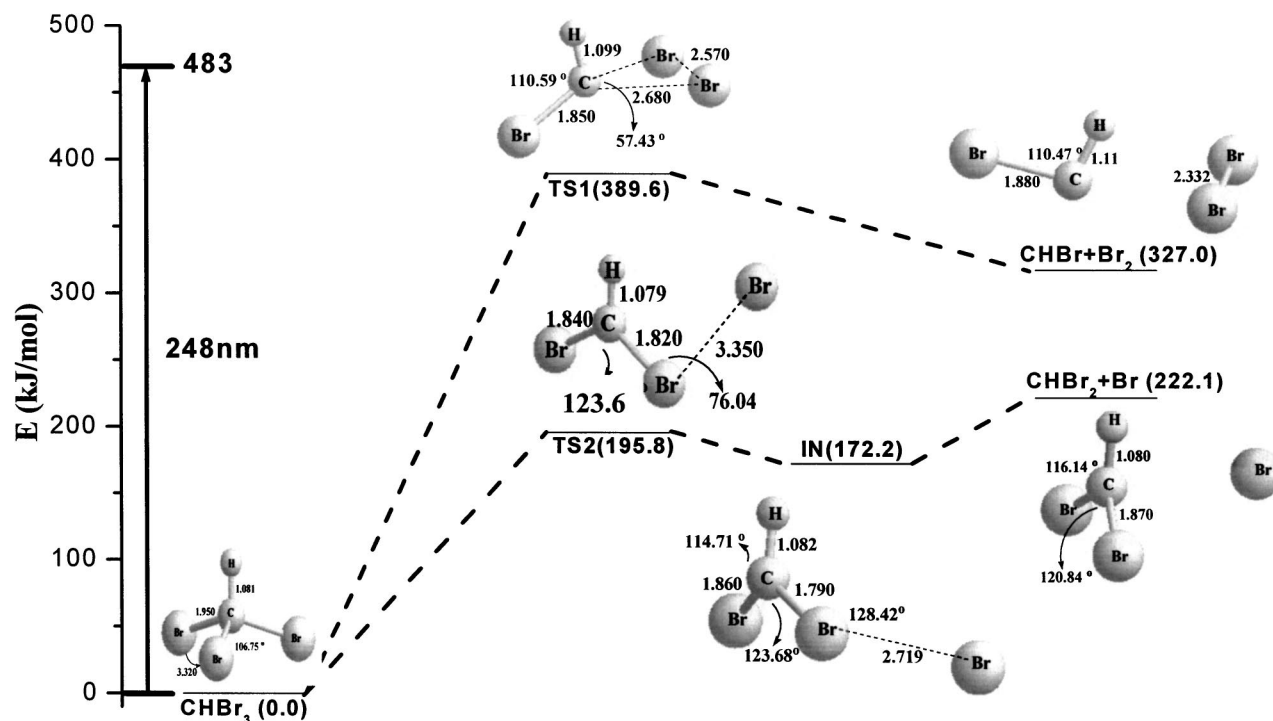


FIG. 6. *Ab initio* state energy calculations of bromoform dissociation along an adiabatic reaction coordinate. Two dissociation channels are calculated, the one leading to $\text{CHBr} + \text{Br}_2$ via a transition barrier 389.6 kJ/mol and the other leading to $\text{CHBr}_2 + \text{Br}$ via a transition barrier 195.8 kJ/mol.

istry of bromine, which has been ignored in the past atmospheric models.

C. Photodissociation pathway

According to *ab initio* calculations, shown in Fig. 6, the energy barrier leading to the fragments CHBr and Br_2 amounts to 389.6 kJ/mol, with respect to the electronic ground state of bromoform. The transition state lies along an adiabatic reaction coordinate for a photodissociation channel on the ground state surface bromoform that leads to the $\text{CHBr} + \text{Br}_2$ products. This part of the surface is characterized by A' symmetry, and its structure has two C-Br bonds elongated to 2.680 Å relative to 1.950 Å in the ground state. The Br-C-Br angle is bent symmetrically with respect to a mirror plane, and the Br··Br is separated by 2.570 Å about 10% larger than 2.332 Å in the ground state Br_2 . Thus the photodissociation pathway via the transition state should lead to a vibrationally hot Br_2 fragment.

According to the *ab initio* potential energy calculations by Peterson and Francisco,¹⁵ the \tilde{A}'^1A_2 , \tilde{B}'^1E , and \tilde{C}'^1A_1 states are probably excited by the laser at 248 nm. The transition $\tilde{A}'^1A_2 \leftarrow \tilde{X}'^1A_1$ is dipole forbidden, but the transitions $\tilde{B}'^1E \leftarrow \tilde{X}'^1A_1$ and $\tilde{C}'^1A_1 \leftarrow \tilde{X}'^1A_1$ are allowed and the ratio of the corresponding transition probability is 50:1. The excited states \tilde{B}'^1E and \tilde{C}'^1A_1 have the correct symmetry to correlate with the fragmented products via the molecular elimination pathway. If the photodissociation occurs directly from a repulsive limb of the excited state, the available energy is anticipated to substantially partition into the translational states of the fragments. On the other hand, the excited states may couple to the high vibrational levels of the ground state via

internal conversion. In this manner, the prolonged lifetime of photodissociation through the $\tilde{B}'^1E - \tilde{X}'^1A_1$ or $\tilde{C}'^1A_1 - \tilde{X}'^1A_1$ couplings should cause a large fraction of the available energy to partition in vibrational levels of the fragments. The vibrationally hot Br_2 fragment observed in the CHBr_3 photolysis at 248 nm seems to favor the dissociation pathway from the highly vibrational levels of the ground state, although the information for the partition of translational energy is not yet known.

Bromoform excited at 248 nm has an energy of 483 kJ/mol, which is enough to readily surpass the transition barrier. As shown in Fig. 7, the elongation of both C-Br bonds in the transition state may break concurrently along a symmetry plane. Thus a concerted mechanism is anticipated in any photolysis. We failed to find the possibility for a stepwise dissociation in the calculations. That is, a free Br atom re-

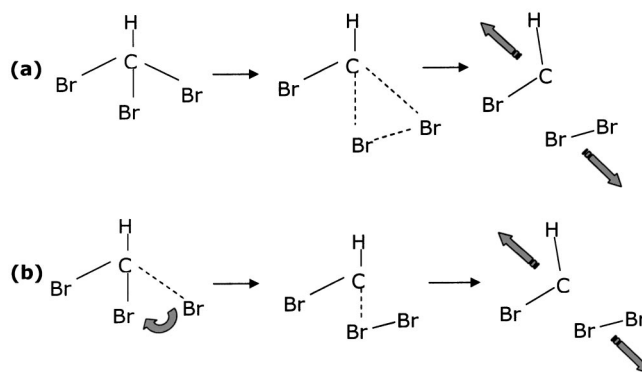


FIG. 7. Photodissociation mechanisms proposed for the Br_2 elimination reaction. (a) concerted dissociation and (b) stepwise dissociation.

sulting from one C-Br bond cleavage moves to form a Br-Br bond before the other C-Br₂ bond breaks (Fig. 7).²⁶ In this manner, the obtained Br₂ fragment may be produced rotationally hot but vibrationally cool. Our theoretical calculations suggest that as long as the single C-Br bond is elongated, the products CHBr₂ and Br are readily obtained through a transition barrier 195.8 kJ/mol, about a half of that encountered in the molecular elimination reaction (Fig. 6).

In a similar photolysis study using velocity ion-imaging detection, Jackson's group have determined an anisotropy parameter β and the translational energy distribution of the other moiety CHBr produced by molecular elimination at 234 and 267 nm, respectively.⁸ Presuming these two primary photodissociation processes originate directly from a repulsive potential surface, then an impulsive model may be applied to predict how the available energy is partitioned in the photofragments.^{27,28} According to this model, the fraction of the available energy E_{avail} partitioned into the product translation, E_T , is given by

$$E_T = \left(\frac{u_{\alpha-\beta}}{u_{A-B}} \right) E_{\text{avail}}, \quad (9)$$

where $u_{\alpha-\beta}$ is the reduced mass of C and Br₂, u_{A-B} is the reduced mass of CHBr and Br₂. The available energies are 511.4 and 448.2 kJ/mol in 234 and 267 nm photolysis, respectively. Thus with this model the average translational energies are predicted to be 30.9 and 18.9 kJ/mol, respectively. The theoretical translational energy for CHBr are estimated to be 19.5 and 12.0 kJ/mol at 234 and 267 nm, respectively. In contrast, the observed translational energy of CHBr peaked at 10 and 20–25 kJ/mol, and the corresponding anisotropic parameter β was measured to be ~ 0 and ~ 0.5 in 234 and 267 nm photolysis, respectively.⁸ The bromoform photolysis at 234 and 267 nm should apparently lead to different dissociation pathways. Xu *et al.* suggested that the pathway differences at these two wavelengths is probably related to the nature of the excited states, but they did not have any further discussion.⁸ According to the theoretical calculations, the \tilde{a}^3A_2 state may be excited at 267 nm, while \tilde{A}^1A_2 , \tilde{B}^1E , and \tilde{C}^1A_1 states are probably excited at 234 nm.¹⁵ The transition probability to the \tilde{a}^3A_2 is weak and it is symmetry forbidden to dissociation via the molecular elimination reaction. However, it can borrow intensity from the nearby \tilde{b}^3E and \tilde{c}^3A_1 triplet states which have relatively larger transition probabilities by 4 and 30 times, respectively, and these surfaces are allowed for reaction. If bromoform dissociates via $\tilde{b}^3E \leftarrow \tilde{X}^1A_1$ perpendicular transition, the recoil fragment relative to the transition dipole would give rise to a negative β value,⁷ which does not agree with the observed average value of 0.5. Thus, the 267 nm photolysis may probably undergo fast direct photodissociation from the repulsive limb of excited state \tilde{c}^3A_1 . In contrast, when photolysis occurs at 234 nm, the measured translational energy of CHBr is far less than that predicted by the impulsive model. A large fraction of the available energy should be partitioned into the vibrational levels of the fragments. As with the photolysis at 248 nm, the excited states \tilde{B}^1E or \tilde{C}^1A_1 of bromoform may have chance to couple with high

vibrational levels of the ground state such that a prolonged lifetime of dissociation may cause the recoil fragments isotropic relative to a transition dipole, yielding a zero β value. Otherwise, the fragment with a nonzero β and a large translational energy would be anticipated as a result of direct photodissociation.

By analyzing ultraviolet resonance Raman spectra of bromoform in cyclohexane solution, Phillips and coworkers found significant intensity in the overtones of nominal Br-C-Br symmetric bend (ν_6), H-C-Br asymmetric bend (ν_3), Br-C-Br symmetric stretch (ν_2), and Br-C-Br asymmetric stretch (ν_5) vibrational modes.²⁹ The lack of strong combination between these four Franck-Condon active modes suggests that more than one electronic transition contribute to the resonance Raman spectra. This seems to suggest that these four active modes in the Raman spectra are related to the two major primary dissociation channels via single Br atom cleavage and Br₂ molecular elimination. Electronic transition that involves short-time dynamics along the ν_5 asymmetric stretch or ν_3 asymmetric bend may lead to the CHBr₂ and Br fragments, while the transition involving the pathways along ν_6 symmetric bend or ν_2 symmetric stretch modes probably result in the Br₂ elimination. In contrast to this viewpoint, Phillips and coworkers related the observed four active modes to the secondary HBr elimination or C-Br bond breaking, by considering scheme (1) as the only channel present in the photolysis with ultraviolet radiation.²⁹ For instance, they anticipated the electronic transition involving the ν_3 H-C-Br asymmetric bend mode to correlate with the secondary HBr elimination reaction. There is no available information to support their speculation regarding this molecular elimination process.

V. CONCLUSION

By using CRDS technique, we have observed the Br₂ molecular elimination as a second major reaction channel following the photodissociation of CHBr₃ at 248 nm. The nascent vibrational spectra of the Br₂ fragment was reported, showing the fragmented Br₂ was vibrationally hot. The quantum yield for this reaction channel was determined to be 0.23 ± 0.05 , consistent with those reported by Jackson and coworkers using velocity ion-imaging detection in the 234 and 267 nm photolysis. With the aid of the calculations by Peterson and Francisco on the low-lying electronic states and the theoretical state structure calculations of the transition along the adiabatic reaction coordinate on the ground state surface in this work, a plausible photodissociation pathway is proposed. The \tilde{A}^1A_2 , \tilde{B}^1E , and \tilde{C}^1A_1 singlet states of bromoform are probably excited at 248 nm. These states may couple to the high vibrational levels of the ground state X^1A_1 , from which the excited bromoform feasibly surpasses a reaction barrier prior to decomposition. The transition state structure tends to correlate with vibrationally hot levels of Br₂ fragment. In addition, a concerted mechanism of photodissociation is anticipated, since two C-Br bonds elongate in the transition state and may break concurrently along a symmetry plane. The observed vibrationally hot Br₂ fragment seems to favor the dissociation pathway from these high vi-

brational levels of the ground state. Nevertheless, the other reaction channel leading to a direct impulsive dissociation from the excited state can not be excluded.

ACKNOWLEDGMENT

This work was supported by National Science Council of Republic of China under Contract no. NSC92-2113-M-002-046.

- ¹R. R. Garcia and S. Solomon, *J. Geophys. Res.*, [Atmos.] **99**, 12937 (1994).
- ²J. H. Butler, *Geophys. Res. Lett.* **21**, 185 (1994).
- ³J. M. Lobert, J. H. Butler, S. A. Montzke, L. S. Geller, R. C. Myers, and J. W. Elkins, *Science* **267**, 1002 (1995).
- ⁴V. L. Dvortsov, M. A. Geller, S. Solomon, S. M. Schaffler, E. L. Atlas, and D. R. Blake, *Geophys. Res. Lett.* **26**, 1699 (1999).
- ⁵W. B. DeMore, *J. Phys. Chem. A* **100**, 5813 (1996).
- ⁶J. P. Simons and A. J. Yarwood, *Trans. Faraday Soc.* **57**, 2167 (1961).
- ⁷W. S. McGivern, O. Sorkhabi, A. G. Suits, A. Derecskei-Kovacs, and S. W. North, *J. Phys. Chem. A* **104**, 10085 (2000).
- ⁸D. Xu, J. S. Francisco, J. Huang, and W. M. Jackson, *J. Chem. Phys.* **117**, 2578 (2002).
- ⁹A. O'Keefe and D. A. G. Deacon, *Rev. Sci. Instrum.* **59**, 2544 (1988).
- ¹⁰A. O'Keefe, J. J. Scherer, A. L. Cooksy, R. Sheeks, J. Heath, and R. J. Saykally, *Chem. Phys. Lett.* **173**, 214 (1990).
- ¹¹D. J. Benard and K. B. Winker, *J. Appl. Phys.* **69**, 2805 (1991).
- ¹²J. Pearson, A. J. Orr-Ewing, M. N. R. Ashfold, and R. N. Dixon, *J. Chem. Phys.* **106**, 5850 (1997).
- ¹³U. Lommatzsch, E. H. Wahl, T. G. Owano, C. H. Kruger, and R. N. Zare, *Chem. Phys. Lett.* **320**, 339 (2000).
- ¹⁴J. J. Scherer, J. B. Paul, A. O'Keefe, and R. J. Saykally, *Chem. Rev.* (Washington, D.C.) **97**, 25 (1997).
- ¹⁵K. A. Peterson and J. S. Francisco, *J. Chem. Phys.* **117**, 6103 (2002).
- ¹⁶A. D. Becke, *J. Chem. Phys.* **98**, 5648 (1993).
- ¹⁷C. Lee, W. Yang, and R. G. Parr, *Phys. Rev. B* **37**, 785 (1988).
- ¹⁸C. Gonzalez and H. B. Schlegel, *J. Phys. Chem.* **94**, 5523 (1990).
- ¹⁹M. J. Frisch, G. W. Trucks, H. B. Schlegel *et al.*, GAUSSIAN 98, Gaussian 98 FULL REF, Gaussian, Inc., Pittsburgh, PA, 2001.
- ²⁰R. F. Barrow, T. C. Clark, J. A. Coxon, and K. K. Yee, *J. Mol. Spectrosc.* **51**, 428 (1974).
- ²¹J. A. Coxon, *J. Quant. Spectrosc. Radiat. Transf.* **12**, 639 (1971).
- ²²I. D. Hein, Database for Excitation-Emission-Spectra (EES) in Combustion Research, http://www.ltk.mw.tu-muenchen.de/wwwlaser/AES/aes_home.htm
- ²³H. K. Haugen, E. Weitz, and S. R. Leone, *J. Chem. Phys.* **83**, 3402 (1985).
- ²⁴J. Tellinghuisen, *J. Chem. Phys.* **115**, 10417 (2001).
- ²⁵R. Atkinson, D. L. Baulch, R. A. Cox, R. F. Hampson, J. A. Kerr, M. J. Rossi, and J. Troe, *J. Phys. Chem. Ref. Data* **26**, 521 (1997).
- ²⁶Q. Zhang, U. Marvet, and M. Dantus, *J. Chem. Phys.* **109**, 4428 (1998).
- ²⁷T. Baer and W. L. Hase, *Unimolecular Reaction Dynamics* (Oxford University Press, New York, 1996), Chap. 9, pp. 361–363.
- ²⁸R. Schinke, *Photodissociation Dynamics: Spectroscopy and Fragmentation of Small Polyatomic Molecules* (Cambridge University Press, New York, 1993), Chap. 10, pp. 251–255.
- ²⁹Y. L. Li, C. W. Lee, K. H. Leung, G. Z. He, and D. L. Phillips, *Mol. Phys.* **100**, 2659 (2002).